A PROOF OF THE STRONG PAPADIMITRIOU–RATAJCZAK CONJECTURE

LECH MAZUR

Abstract. We prove the strong Papadimitriou–Ratajczak conjecture: every finite simple 3-connected plane graph admits a convex greedy straight-line drawing. The drawing preserves the prescribed embedding and outer face, and all facial polygons are strictly convex. We first construct an injective integer height labeling with greedy progress along original edges. The induction is carried out on rooted strong-circuit graphs and preserves greediness after deletion of the minimum vertex. Positive, possibly asymmetric local weights make these heights harmonic; solving the corresponding horizontal equations places the drawing in a strip of width one quarter. A rooted-forest identity gives strict facial supports, and a geometric assembly argument identifies the resulting polygons with the complementary faces. The same drawing has Euclidean greedy progress at least three quarters in this normalization. An accompanying Lean 4 formalization proves the existence theorem from the original continuous embedding and three-connectivity assumptions.

1. Introduction

A drawing $q : V(G) \to \mathbb{R}^2$ of a finite graph is *greedy* if, for every pair of distinct vertices s, t, there is a neighbor a of s such that

$$\|q(t) - q(a)\| < \|q(t) - q(s)\|.$$

Here and throughout, the norm is Euclidean. Greedy routing uses this condition to choose the next edge using only the destination and the current neighbors. Strict decrease of distance prevents a repeated vertex, so every such sequence of choices reaches its destination.

Papadimitriou and Ratajczak formulated two conjectures in their 2004 paper on geometric routing [8]: every 3-connected planar graph admits a greedy drawing, and every such graph admits a convex greedy drawing. Leighton and Moitra proved the first conjecture in 2008 [6]. Da Lozzo, D'Angelo and Frati later established the existence of planar greedy drawings [2]. We prove the convex version, usually called the *strong Papadimitriou–Ratajczak conjecture*, while preserving an arbitrary prescribed plane embedding and its outer face.

1.1. Conventions and main result.

All graphs are finite, simple and undirected. A graph is 3-connected if it has at least four vertices and remains connected after deletion of any set of at most two vertices. A plane graph includes an embedding by distinct vertex points and continuous simple edge arcs, with exactly their prescribed endpoint incidences. Its faces are the connected components of the complement, and its outer face is the unbounded component. The edge arcs need not be straight. For a 2-connected plane graph, every facial boundary is a simple cycle; we use the standard planar graph conventions in [3].

A straight-line drawing has distinct vertex positions, no vertex in the open segment of an edge, and no intersection of distinct edge segments except at a common endpoint. A facial polygon is the boundary of a complementary face. For the outer face, convexity refers to the bounded polygon enclosed by its boundary. We use *strictly convex polygon* in the polygonal sense: the polygon is simple, encloses a bounded convex body with nonempty interior, and every directed edge puts every other polygon vertex strictly on its inner side. In particular, consecutive sides

Date: September 9, 2026.

2020 *Mathematics Subject Classification.* Primary 05C10; Secondary 05C85.

Key words and phrases. Convex greedy drawing, plane graph, geometric routing, integer heights, rooted forest, formal verification, Lean.

are not collinear. This terminology does not assert that the closed body is strictly convex as a subset of $\mathbb{R}^2$.

Theorem 1 (strong Papadimitriou–Ratajczak conjecture)**.** *Every finite simple 3-connected plane graph G has an injective straight-line drawing $q : V(G) \to \mathbb{R}^2$ preserving its embedding and outer face, with every facial boundary a strictly convex polygon. The drawing can be normalized so that, for every pair of distinct vertices s, t, some original neighbor a of s satisfies*

$$\|q(t) - q(a)\| + \tfrac{3}{4} \le \|q(t) - q(s)\|.$$

The construction preserves the original vertex and edge identities and the cyclic order of edges at each vertex. In fact, the original embedding is carried to the new one by an orientation-preserving homeomorphism of the plane. No numerical positions are prescribed for the outer vertices. The same chosen neighbor also gives squared-distance decrease at least one. These margins refer to the normalization used in the proof and are not scale-invariant bounds.

1.2. **Proof strategy and relation to earlier work.** The main construction is an injective integer labeling h for which every ordered pair $s \neq t$ has an original neighbor a satisfying

$$|h(t) - h(a)| < |h(t) - h(s)|. \tag{1}$$

The induction uses the rooted strong-circuit decomposition of Da Lozzo, D'Angelo and Frati [2]. Its invariant includes the same greedy property after deletion of the minimum vertex. This extra condition permits two pieces to be joined using original edges while retaining integer progress in both directions. Section 2 states the rooted class, gives the required decomposition in that notation, and proves the induction on this class before applying it to 3-connected graphs.

The geometric step uses positive convex-combination equations. Tutte's equilibrium theorem [9] and its asymmetric extensions, including the work of Floater [5] and Ó Dúnlaing [7], provide the relevant classical setting; see also the formulation in Erickson and Lin [4]. Our use of unequal weights in the two directions of an edge is within this established theory. We choose the weights to make the previously constructed heights harmonic, prescribe the outer horizontal coordinates on a narrow concave arc, and solve the same equations for the remaining horizontal coordinates. The maximum principle places all points in $0 \le X \le 1/4$.

For completeness, we prove the geometric properties of these coordinates directly. Section 4 derives a signed-area identity from a rooted-forest expansion, in the tradition of the matrix-tree theorem [1]. Three-connectivity and planar path order make each required facial area strictly positive. Section 5 then proves that the resulting individual polygons tile the outer polygon, that no extra edge or vertex contacts occur, and that these polygons are precisely the complementary faces with the prescribed embedding.

Finally, any strict decrease in an integer height gap is at least one. Horizontal motion in a strip of width one quarter costs at most one quarter in the elementary distance estimate of Section 6. Thus the geometric construction retains the greedy progress already supplied by (1). Section 7 describes the accompanying Lean formalization and its relation to the proof.

2. Rooted integer heights

The inductive statement is stronger than the assertion needed for a 3-connected graph. It applies to the rooted pieces of a decomposition and retains greediness after deletion of their first root. This section states that invariant before applying induction.

2.1. **The structural input.** Let J be a 2-connected plane graph and let u, v be distinct vertices of its outer cycle. Write $O(J)$ for the outer vertices, and $\tau_{uv}(J)$, $\beta_{uv}(J)$ for the clockwise and counterclockwise outer paths from u to v, respectively. A vertex 2-cut is a pair $S = \{a, b\}$ for which $J - S$ is disconnected.

Definition 2 (Rooted strong-circuit graph)**.** We write $\mathcal{S}(J; u, v)$ if J is the single edge uv, or if J is 2-connected with at least three vertices, $u, v \in O(J)$ are distinct, and the following conditions hold:

(i) If $uv \in E(J)$, then $\tau_{uv}(J)$ consists of that edge.

(ii) Every vertex 2-cut S satisfies

$$S \subseteq O(J), \qquad S \cap (V(\beta_{uv}(J)) \setminus \{u, v\}) \neq \varnothing,$$

and every component of $J - S$ contains a vertex of $O(J)$.

The outer vertex in the last clause is a surviving vertex, since the vertices of S have been deleted. This is the strong-circuit class of Da Lozzo, D'Angelo and Frati [2, Definition 4].

Definition 3 (Series chain)**.** An endpoint-rooted series chain from r_0 to r_k, $k \geq 1$, is a sequence $\mathcal{S}(J_i; r_{i-1}, r_i)$, $1 \leq i \leq k$, in which consecutive blocks meet precisely at the indicated common root and nonconsecutive blocks are vertex-disjoint. Its graph is the union of these blocks. A one-block chain and single-edge blocks are allowed.

The union of a series chain need not be 2-connected. Whenever a graph is deleted or restricted below, all remaining edges retain their original adjacency; no auxiliary edge is available for routing.

Proposition 4 (Rooted decomposition)**.** *Suppose $\mathcal{S}(J; u, v)$, and J is neither an edge nor a cycle. Then the following alternatives hold.*

(a) *If $uv \in E(J)$, then $J - uv$ is a series chain from u to v.*

(b) *If $uv \notin E(J)$, there are plane subgraphs $H, K \subseteq J$, with their inherited embeddings, such that $\mathcal{S}(H; u, a)$ holds and K is an endpoint-rooted series chain from z to v, satisfying*

$$u, a, z \text{ are distinct}, \quad v \notin V(H), \quad V(H) \cap V(K) = \{z\}, \quad V(H) \cup V(K) = V(J).$$

In particular, $E(H) \cup E(K) \subseteq E(J)$. The edge av belongs to J, and

$$E(J) \setminus (E(H) \cup E(K) \cup \{av\}) \subseteq \{vy : y \in V(H)\}.$$

Every strong-circuit subgraph in either decomposition has fewer edges than J.

This is the original-subgraph form of [2, Lemmas 5–6]. For clarity, we give the identification of the objects used here with those in that source. In the missing-edge case, H is the block of $J - v$ containing u; its roots and the attachment are $a = y_1$, $z = y_\ell$, and K is the last bridge B_ℓ. Properties 6a–6b leave only the last bridge potentially nontrivial, 6d gives av, 6e places z strictly inside $\beta_{u,a}(H)$, and 6g–6h give the rooted subgraphs. These properties give the displayed vertex-set intersection, coverage and edge inclusion. The edge uv in case (a), or av in case (b), is absent from those subgraphs, which gives strict descent in edge count.

One detail of this adaptation concerns the last bridge. The cited proof may temporarily adjoin zv to it and then apply the root-edge decomposition. If the augmented graph is a cycle, deletion of the added edge leaves a z-to-v path; its individual edges are the required series blocks. If the last bridge is itself the original edge zv, it is a one-block chain. Thus the chain consists entirely of original edges in either case. The cited decomposition, including these exceptional cases, is the structural input to the proof.

Lemma 5 (Three-connected graphs and cycles)**.** *A 3-connected plane graph, rooted at a clockwise outer edge uv, belongs to $\mathcal{S}$. A cycle in $\mathcal{S}(J; u, v)$ has adjacent roots.*

Proof. A 3-connected graph has no vertex 2-cuts, so the cut conditions are vacuous. The chosen outer edge has the required orientation. If the roots of a cycle were nonadjacent, deleting $\{u, v\}$ would disconnect the cycle, but neither member of this cut is internal to β_{uv}. This contradicts Definition 2. □

2.2. **The induction invariant.** For a graph J, an injective map $h : V(J) \to \mathbb{Z}$ is *greedy in height* if

$$\forall s \neq t \quad \exists a \in N_J(s) \quad |h(t) - h(a)| < |h(t) - h(s)|. \tag{2}$$

Here and below a restriction of h uses the same numerical values.

Definition 6 (Rooted greedy labeling)**.** For distinct roots u, v, a rooted greedy labeling of $(J; u, v)$ is an injective integer labeling h such that

(i) $h(u) = 0$ is the minimum, and $h(v) = T > 0$ is the maximum;
(ii) the least positive value of h is 1;
(iii) h is greedy in height on both J and $J - u$.

A graph with one surviving vertex satisfies the last greediness condition vacuously.

Lemma 7 (Elementary consequences)**.** *In a finite graph with a greedy injective labeling, every vertex other than the maximum has a higher neighbor, and every vertex other than the minimum has a lower neighbor. The minimum is adjacent to the vertex with the next smallest height. Greediness is preserved by translation of all heights and by adding edges on the same vertex set.*

Proof. Use the maximum as target in (2). Since every height is at most that maximum, a strict improvement from a nonmaximum vertex must have larger height. The minimum gives the lower-neighbor assertion. If r has the least height above the minimum u, use u as target from r. Its improving neighbor has smaller height, so it must be u. Translation leaves every height difference unchanged, and adding edges preserves every improving edge. □

Lemma 8 (Series pasting)**.** *If every block of a series chain has a rooted greedy labeling, then their translated labelings give a rooted greedy labeling of the chain.*

Proof. Let h_i have span $T_i = h_i(r_i) > 0$, and put $A_i = \sum_{j<i} T_j$. On J_i, set $h = A_i + h_i$. The two definitions at the shared root agree. The intervals $[A_i, A_i + T_i]$ meet only at consecutive endpoints, whose vertices are already identified. Thus the labeling is injective, its roots are the extrema, and its first positive value is 1.

If source and target belong to one block, use an improving neighbor within that block. Otherwise, a source strictly inside a block has a higher or lower neighbor within the same block in the direction of the target, by Lemma 7. This neighbor stays between the source height and the height interval of the target's block, so it strictly improves the absolute difference. At a shared root choose the block on the target's side and use its inward neighbor. These cases also cover targets that are shared roots.

After deleting r_0, use the greedy restriction to $J_1 - r_0$ on the first block, and the unchanged labelings on later blocks. The same interval comparisons apply. If $J_1 - r_0$ is a singleton, its vertex is r_1; it uses the next block for a target outside that singleton. If there is no next block, there are no distinct surviving source-target pairs. This proves the deletion condition. □

Lemma 9 (Joining two height ranges)**.** *Assume the vertex and edge conditions of Proposition 4(b). If H, rooted at u, a, and K, rooted at z, v, have rooted greedy labelings, then their union together with the original edge av has such a labeling, rooted at u, v.*

Proof. Write the lower labeling as f, with $f(u) = 0$, $f(a) = A$ and $f(z) = c$. Injectivity and the distinctness of u, a, z give $0 < c < A$. Let g be the labeling of the upper chain. If r is its first vertex above z, then $g(r) = 1$, and rz is an original edge by Lemma 7. On $K - z$, put

$$k(x) = g(x) - g(r), \qquad W = k(v) \geq 0.$$

This restriction is greedy, has minimum $k(r) = 0$, and has maximum W. Choose

$$D = \begin{cases} 1, & W = 0, \\ 1 + \max\{A - c, W\}, & W > 0, \end{cases} \qquad h(x) = \begin{cases} f(x), & x \in V(H), \\ A + D + k(x), & x \in V(K) \setminus \{z\}. \end{cases} \tag{3}$$

The two height ranges are disjoint. The global minimum is u, the maximum is v, and the first positive height remains the first positive height of H, namely 1.

For $W > 0$, sources and targets in one range use the greediness of H or of $K - z$. Suppose next that the source is in H and the target t is in $K - z$. If the source is not a, a higher neighbor in H lies closer to every upper target. At a, use the edge av; its new distance is $W - k(t)$ and its old distance is $D + k(t)$. The required strict inequality follows from $D > W$ and $k(t) \geq 0$.

Conversely, let the target have lower height $y \in [0, A]$. An upper source other than r has a lower neighbor in $K - z$, which remains above every lower target and therefore improves. At r, use rz. The comparison is

$$|y - c| < A + D - y,$$

because

$$y + |y - c| \leq 2A - c < A + D. \tag{4}$$

For $y \leq c$ the left side equals $c \leq 2A - c$; for $y \geq c$ it equals $2y - c \leq 2A - c$. The last strict inequality uses $D > A - c$. This exhausts all source-target pairs.

After deletion of u, the same argument uses the greedy restriction to $H - u$ for lower-range pairs and for a higher neighbor toward a. The edge rz survives because $z \neq u$; av also survives. Thus all improving edges between the ranges remain available.

Finally, $W = 0$ means $K - z = \{v\}$, by injectivity. At a lower source different from a, take a higher neighbor toward a. At a, take v. From v toward a lower target of height y, take a: the distance falls from $A + 1 - y$ to $A - y$. Within H use its improving neighbors. This argument remains valid in $H - u$, proving the singleton case as well. □

Proposition 10 (Rooted height construction)**.** *Every $\mathcal{S}(J; u, v)$ admits a rooted greedy labeling. Consequently every endpoint-rooted series chain of strong-circuit graphs admits one.*

Proof. Induct on $|E(J)|$ within the full class $\mathcal{S}$. For a single edge use heights $0, 1$. By Lemma 5, a cycle in the class has adjacent roots. Label the other u-to-v path by consecutive integers starting at 0. Its consecutive edges give height progress; after deleting u, its remaining path gives the same progress and the maximum remains v.

For a nonterminal graph, apply Proposition 4. Each strong-circuit subgraph is smaller in edge count, so the induction hypothesis applies to every such subgraph. In case (a), paste their labelings using Lemma 8, then restore uv. In case (b), first paste the blocks of K, then apply Lemma 9 to H and K. Restore the remaining original edges in either case; by Lemma 7, all improving edges remain available. This proves the assertion for strong-circuit graphs. Its series-chain consequence follows from Lemma 8. □

Corollary 11 (Heights for the main theorem)**.** *For any clockwise outer edge uv of a 3-connected plane graph, there are injective integer heights with minimum $h(u) = 0$, maximum $h(v) = T > 0$, least positive height 1, and greediness on both G and $G - u$.*

Proof. Apply Lemma 5 and Proposition 10. □

For example, the join with $A = 4$, $c = 2$ and $W = 3$ uses $D = 4$. The ranges are $[0, 4]$ and $[8, 11]$. For an upper target $8 + k$, the edge from height 4 to height 11 improves because $3 - k < 4 + k$. For a lower target $y \in [0, 4]$, the edge from height 8 to height 2 improves because $y + |y - 2| \leq 6 < 8$. Figure 1 shows these two cross-range edges.

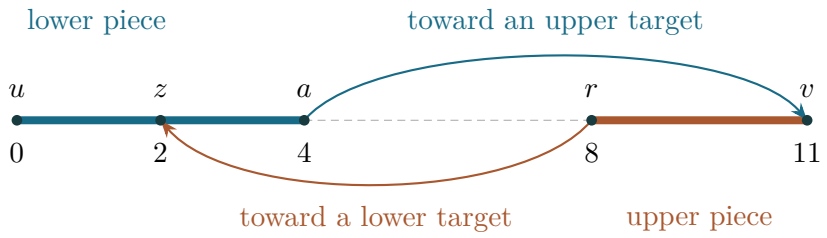

FIGURE 1. A join with $A = 4$, $c = 2$, $W = 3$, and $D = 4$. The arrows show the two original edges used for cross-range progress. The horizontal axis records height values.

2.3. **Boundary order in the original embedding.** We next recover the height order on the outer path from the given embedding. This avoids imposing an additional boundary-order hypothesis on the inductive labeling.

Lemma 12 (Facial height order)**.** *Orient every edge of G toward its higher endpoint. At every vertex other than u, v, the incoming edges form one nonempty interval in the cyclic order and the outgoing edges form the other. Every facial cycle has a unique minimum and a unique maximum, and splits into two increasing paths between them. The outer cycle has extrema u, v.*

Proof. Every nonextreme vertex has both kinds of incident edge by Lemma 7. For a vertex s, let σ_s be the number of changes between incoming and outgoing edges in its cyclic order. For a face F, let k_F be the number of local minima of height around its boundary. Injectivity excludes equal-height endpoints, and local minima and maxima alternate along each cyclic boundary, so there are $2k_F$ facial extrema.

At a vertex corner, either the two darts have opposite directions relative to the vertex, giving one change counted in σ_s, or they have the same direction, giving a minimum or maximum of the incident face. The total number of corners is $2m$, where $m = |E(G)|$. Writing $n = |V(G)|$ and f for the number of faces including the outer face gives

$$2m = \sum_s \sigma_s + 2\sum_F k_F, \qquad n - m + f = 2.$$

The extrema u, v have $\sigma_u = \sigma_v = 0$; every other σ_s is at least 2, and every k_F is at least 1. Subtraction yields

$$\sum_{s \neq u,v} (\sigma_s - 2) + 2\sum_F (k_F - 1) = 0.$$

All summands are nonnegative, hence all vanish. Two changes give exactly the stated incoming and outgoing intervals. A unique local minimum and maximum on a cycle give its two strictly increasing sides. On the outer cycle, the globally extreme vertices u, v are present, so they are its extrema. □

3. Positive equations with the prescribed heights

Fix the heights from Corollary 11 and their root edge uv. Let $B \subseteq V(G)$ be the vertices of the original outer cycle and $I = V(G) \setminus B$. We choose directed positive weights so that the height function itself satisfies the interior equilibrium equations.

For $s \in I$, define

$$P_s = \sum_{t \in N_G(s)} \max\{h(t) - h(s), 0\}, \qquad N_s = \sum_{t \in N_G(s)} \max\{h(s) - h(t), 0\}.$$

Both are positive integers, because an interior vertex is neither global extremum and therefore has neighbors in both height directions. A *dart* st denotes the edge st directed from s to t. Set $w_{ss} = 0$, set $w_{st} = 0$ for nonadjacent distinct vertices, and on original darts set

$$w_{st} = \begin{cases} N_s, & s \in I,\ h(t) > h(s), \\ P_s, & s \in I,\ h(t) < h(s), \\ 1, & s \in B. \end{cases} \tag{5}$$

All original dart weights are positive. They need not satisfy $w_{st} = w_{ts}$. For a function f on the vertices write

$$(Lf)(s) = \sum_t w_{st}\big(f(s) - f(t)\big).$$

The upward differences in Lh contribute $-N_s P_s$, and the downward differences contribute $P_s N_s$; hence

$$(Lh)(s) = 0 \qquad (s \in I). \tag{6}$$

Dividing by $\sum_t w_{st} > 0$ expresses $h(s)$ as an average of its neighbors' heights with positive coefficients. The horizontal coordinate will use the same coefficients.

Lemma 13 (Dirichlet problem)**.** *For boundary data $b : B \to \mathbb{Q}$, there is a unique function $X : V(G) \to \mathbb{Q}$ with $X|_B = b$ and $LX = 0$ on I. Moreover*

$$\min_{z\in B} b(z) \le X(s) \le \max_{z\in B} b(z) \qquad (s \in V(G)).$$

Proof. Fix an ordering of the finite vertex set. Let e_s denote its coordinate row vector and define the square matrix M by

$$M_{s,*} = \begin{cases} e_s, & s \in B, \\ \sum_t w_{st}(e_s - e_t), & s \in I. \end{cases} \tag{7}$$

The equations are $MX = c$, where $c(s) = b(s)$ for $s \in B$ and $c(s) = 0$ otherwise.

Suppose first that $Mf = 0$ over $\mathbb{R}$. Then $f = 0$ on B. If f has a positive maximum at an interior vertex s, all summands $w_{st}(f(s) - f(t))$ are nonnegative. Their sum is zero, so every neighbor of s has that same maximum. Connectedness supplies a path from s to B; propagation along this path contradicts the zero boundary values. Applying the argument to $-f$ excludes a negative minimum. Thus M has trivial kernel and is invertible. Its entries and c are rational, so the unique solution is rational. The same propagation argument, applied to any maximum exceeding the boundary maximum or minimum below the boundary minimum, proves the stated bounds. □

Choose the particular boundary values

$$\phi(y) = \frac{y(T-y)}{T^2}, \qquad X(b) = \phi(h(b)) \quad (b \in B), \qquad q(s) = (X(s), h(s)). \tag{8}$$

By Lemma 13, $0 \le X(s) \le 1/4$ for all s. Both coordinates of q satisfy the same interior equations, by construction and (6). The placement is injective because the heights are injective.

Lemma 14 (The outer polygon)**.** *The points $q(b)$, $b \in B$, in their original counterclockwise outer-cycle order, form a strictly convex polygon.*

Proof. The clockwise root path is the single edge uv. Lemma 12 makes the other u-to-v path strictly increasing in height. Its points lie on $x = \phi(y)$ for $0 \le y \le T$, while the closing segment vu lies on $x = 0$. The chain is simple because its height coordinate is strictly increasing, and its internal points have $x > 0$.

For consecutive heights $a < b$ on the chain, let $\ell_{ab}(y)$ be the affine function interpolating $\phi(a)$ and $\phi(b)$. A direct calculation gives

$$\phi(y) - \ell_{ab}(y) = -\frac{(y-a)(y-b)}{T^2}. \tag{9}$$

Every other boundary height lies outside $[a, b]$, because a, b are consecutive. It follows that the other points lie strictly to the left of the directed segment from $(\phi(a), a)$ to $(\phi(b), b)$: indeed its signed area with $(\phi(y), y)$ is $(b-a)(\ell_{ab}(y) - \phi(y)) > 0$. For the closing edge from height T to height 0, the strict left side is $x > 0$, containing every other point. Thus every boundary edge strictly supports all other boundary vertices. The polygon criterion proved in Lemma 20, which uses only these inequalities, supplies strict convexity. □

The last appeal is to a geometric lemma whose proof is independent of the equilibrium equations and the outer-boundary construction.

3.1. **An exact four-vertex example.** Take K_4 with outer cycle u, b, v, counterclockwise, and interior vertex s. Assign heights $0, 1, 2, 3$ to u, b, s, v, respectively. These are greedy on K_4 and on $K_4 - u$, since any destination is itself a neighbor. Figure 2 gives the coordinates and drawing.

At s, $P_s = 1$ and $N_s = 3$, so the outgoing weights to u, b, v are $1, 1, 3$. The two equations are

$$X(s) = \frac{X(u) + X(b) + 3X(v)}{5} = \frac{2}{45}, \qquad h(s) = \frac{0 + 1 + 3 \cdot 3}{5} = 2.$$

The example exhibits the asymmetric weights explicitly. The forest and planar arguments in the next sections establish strict convexity for the general construction.

Vertex	h	X
u	0	0
b	1	2/9
s	2	2/45
v	3	0

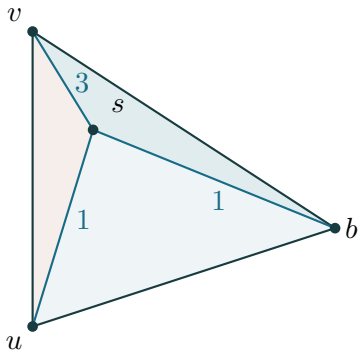

FIGURE 2. The K_4 coordinate construction. Labels on the three interior edges are the outgoing weights from s. The diagram enlarges the horizontal scale; the adjacent table gives the actual coordinates.

4. Forests and strict facial support

This section separates an algebraic identity from its planar application. The determinant expansion applies to positive directed weights without symmetry. Planarity is used only to determine the cyclic order of the three boundary roots associated with a facial triple.

4.1. **A common-forest determinant identity.** Keep the boundary set B, its complement I, and the matrix M of (7). An *outgoing choice* is a map $d : V(G) \to V(G)$ such that $d(b) = b$ on B, and $d(s)$ is an original neighbor of s for $s \in I$. It is *rooted at* B if iteration of d reaches B from every vertex. Write $\mathcal{F}_B$ for the finite set of rooted choices, $r_d(s)$ for the first boundary vertex reached, and

$$W(d) = \prod_{s \in I} w_{s,d(s)}.$$

The empty product is 1. Apart from the fixed boundary loops, these choices are directed forests with one boundary root in each component. The paths to their roots use only original graph edges.

Lemma 15 (Partition determinant)**.** *For the positive weights* (5)*,*

$$Z := \det M = \sum_{d \in \mathcal{F}_B} W(d) > 0.$$

Proof. Expand $\det M$ multilinearly in the rows indexed by I, leaving boundary rows fixed. Each term chooses one neighbor $d(s)$ at each interior vertex. After factoring out $W(d)$, its matrix M_d has boundary rows e_b and interior rows $e_s - e_{d(s)}$.

If an interior directed cycle occurs, the sum of its rows is zero, so the determinant vanishes. Otherwise every successor chain reaches a boundary vertex: a chain in a finite set either reaches B or repeats an interior vertex. Order the vertices by increasing distance along the chosen arrows to B, putting all boundary vertices first. Simultaneously permuting rows and columns to this order leaves the determinant unchanged. Each interior row has its 1 on the diagonal and its -1 in an earlier column. Thus M_d is triangular with diagonal 1, and $\det M_d = 1$.

Finally, a rooted choice exists. Fix each boundary vertex, and at every interior vertex choose a neighbor whose graph distance to B is one smaller. Connectedness and $B \neq \varnothing$ ensure that these choices are possible. Each rooted choice has positive weight, so the partition sum is positive. □

For points $p_0, p_1, p_2 \in \mathbb{R}^2$, set

$$\Delta(p_0, p_1, p_2) = \det(p_1 - p_0, p_2 - p_0).$$

This is twice the signed area of the ordered triangle.

Lemma 16 (Common-forest area identity)**.** *If both coordinates of $q : V(G) \to \mathbb{R}^2$ satisfy the interior equations $Lq = 0$, then, for any ordered triple a_0, a_1, a_2 of vertices, including triples with repetitions,*

$$Z\,\Delta(q(a_0), q(a_1), q(a_2)) = \sum_{d \in \mathcal{F}_B} W(d)\,\Delta(q(r_d(a_0)), q(r_d(a_1)), q(r_d(a_2))). \tag{10}$$

Proof. Let $n = |V(G)|$, and let P be the $n \times 3$ matrix whose row at s is $(1, q_1(s), q_2(s))$. Let C have the same boundary rows as P and zero interior rows. The constant coordinate is harmonic, so $MP = C$. Let E be the $3 \times n$ matrix whose row i is e_{a_i}. Subtracting the first row of EP from its other two rows gives

$$\det(EP) = \Delta(q(a_0), q(a_1), q(a_2)).$$

The block multiplication

$$\begin{pmatrix} M & -C \\ E & 0 \end{pmatrix} \begin{pmatrix} I_n & P \\ 0 & I_3 \end{pmatrix} = \begin{pmatrix} M & 0 \\ E & EP \end{pmatrix}$$

therefore proves

$$\det \begin{pmatrix} M & -C \\ E & 0 \end{pmatrix} = \det M \, \det(EP). \tag{11}$$

The multiplying matrix has determinant 1; no inverse of M is used in this identity.

Expand the upper interior rows of the bordered determinant. Their added three coordinates are zero, so after weights are factored out an interior directed cycle still has zero row sum. For a rooted choice d, let P_d assign to s the row $(1, q_1(r_d(s)), q_2(r_d(s)))$. On a boundary row this equals C; on an interior row, s and $d(s)$ have the same root. Hence $M_d P_d = C$. Applying the same block multiplication with M_d, P_d shows that the unweighted term is $\det M_d \det(EP_d) = \det(EP_d)$. Its value is the signed area of the three boundary roots. Summing these terms proves (10). If a terminal is repeated, the corresponding selected rows repeat on both sides, and the same determinant calculation still applies. □

The algebra belongs to the matrix-tree and all-minors tradition; see Chaiken [1]. We have given the row-oriented bordered expansion to specify its signs, boundary convention and single denominator. For the placement (8), division by Z expresses each signed area as an average of boundary-root areas. The next two lemmas ensure nonnegativity of every term for a facial triple and positivity of at least one term.

4.2. **A five-vertex forest calculation.** The cancellation can be seen in an example with two interior vertices. Start with the outer triangle u, b, v, insert a vertex s adjacent to all three, and insert t in the face u, b, s, adjacent to those three vertices. Assign heights

$$h(u) = 0, \quad h(b) = 1, \quad h(t) = 2, \quad h(s) = 3, \quad h(v) = 4.$$

These heights form a rooted greedy labeling. The only nonadjacent pair is t, v, and s gives strict height progress in both directions; all other pairs use their connecting edge. This remains true after deletion of u.

The boundary coordinates are $X(u) = X(v) = 0$, $X(b) = 3/16$. The weights from s to u, b, t, v are $1, 1, 1, 6$, and the weights from t to u, b, s are $1, 1, 3$. Thus

$$\begin{pmatrix} 9 & -1 \\ -3 & 5 \end{pmatrix} \begin{pmatrix} X(s) \\ X(t) \end{pmatrix} = \begin{pmatrix} 3/16 \\ 3/16 \end{pmatrix}, \qquad X(s) = \frac{3}{112}, \quad X(t) = \frac{3}{56}.$$

There are $4 \cdot 3 = 12$ outgoing choices. Exactly one has an interior directed cycle: $s \mapsto t \mapsto s$, of weight 3. All others are rooted. The total weight of all choices is $9 \cdot 5$, so the partition sum is $Z = 45 - 3 = 42$, the determinant above.

For the facial triple (u, b, t), a nonzero boundary-root area requires t to reach v. This occurs only in the choice $t \mapsto s \mapsto v$, of weight $3 \cdot 6 = 18$. The outer signed area is $\Delta(q(u), q(b), q(v)) = 3/4$, giving

$$\Delta(q(u), q(b), q(t)) = \frac{18(3/4)}{42} = \frac{9}{28}.$$

The same value follows directly from $(3/16) \cdot 2 - (3/56) \cdot 1$. This small calculation illustrates both the vanishing cyclic term and the common-forest area identity.

4.3. **Disjoint paths and their order.** A *first-boundary path* has its last vertex in B and no other vertex in B. If its first vertex belongs to B, it must have length zero. Path disjointness includes endpoints.

Lemma 17 (Three first-boundary paths)**.** *Let B contain at least three vertices of a 3-connected graph. Any three distinct vertices have pairwise vertex-disjoint first-boundary paths to three distinct vertices of B. Every such family extends to a rooted choice in $\mathcal{F}_B$ preserving each of its directed steps.*

Proof. The hypothesis on B holds for the outer cycle in our application. Use the vertex form of the set-to-set Menger theorem [3], allowing a length-zero path when the two terminal sets intersect. Let A be the three specified vertices. A set S of at most two vertices cannot meet every A-to-B path: both $A \setminus S$ and $B \setminus S$ are nonempty, and $G - S$ is connected. If the surviving sets overlap, their common vertex supplies a length-zero path; otherwise connectedness supplies a path between them. Menger's theorem therefore gives three pairwise vertex-disjoint A-to-B paths. Truncate each at its first boundary vertex. Their endpoints remain distinct and their supports remain disjoint.

Orient the three paths toward their boundary endpoints. Fix all boundary vertices. Let U be the union of their supports with B. Every vertex outside U chooses an original neighbor of smaller graph distance to U. Iteration reaches U, and then follows one of the prescribed paths or stays at a boundary vertex. Thus the choice is rooted. It retains all prescribed steps, and its weight is positive because each selected dart has positive weight. □

Lemma 18 (Edge-anchored boundary order)**.** *Let ab be an edge directed counterclockwise around a bounded face of the original plane graph, and let c be another vertex on that facial cycle. Suppose three vertex-disjoint first-boundary paths from a, b, c end at r_a, r_b, r_c. These roots occur in that counterclockwise order on the outer cycle.*

Proof. All paths and faces in this proof lie in the original embedding. If ab is an outer edge, the paths from a, b have length zero. The directed edge ab has the same direction as the counterclockwise boundary of the bounded outer body. Its endpoints are consecutive on that boundary. The distinct third root therefore occurs on the remaining arc from b back to a, as required.

Suppose ab is not an outer edge. Concatenate the reverse of the first path, the original arc ab, and the second path. The result is a simple arc Q from r_a to r_b. Indeed the two path supports are disjoint, neither can pass through the other's starting vertex, and original edge arcs intersect only at their original common endpoints. The interior of Q avoids the outer boundary by the first-boundary property and the assumption on ab. Thus Q is a proper crosscut of the Jordan disk bounded by the outer cycle.

The crosscut separates that disk into two sides. With Q directed from r_a to r_b, its left side is bounded by Q followed by the counterclockwise outer arc from r_b to r_a. The interior of the chosen face in the original embedding is disjoint from Q, since Q uses graph edges, and is connected. Near an interior point of ab, the face is on the left by its prescribed counterclockwise orientation. It therefore lies wholly on the left side of Q.

The point c lies in the closure of that face and is not on Q, by disjointness of the three paths. Its third path also avoids Q. Consequently this path cannot leave the left side before reaching the outer boundary. Its endpoint lies on the outer arc from r_b to r_a, excluding the endpoints because the paths are disjoint. This gives the asserted cyclic order. If c is already on the outer cycle, the path has length zero and the same closure argument locates $c = r_c$ on that arc. No assumption that the face and the outer cycle are otherwise disjoint is used. □

The crosscut separation and side convention are consequences of the Jordan–Schönflies theorem [7, Propositions 1.7 and 1.9]. They concern the original embedding and do not presuppose any noncrossing property of q.

Lemma 19 (Strict facial support)**.** *For every counterclockwise directed edge ab of a bounded face of the original embedding and every other vertex c of that face,*

$$\Delta(q(a), q(b), q(c)) > 0.$$

Proof. Consider the summands in (10) for (a, b, c). Repeated roots give area zero. If the three roots are distinct, the successor paths to them are vertex-disjoint: any two successor paths that meet have identical tails and hence the same root. Their order is therefore given by Lemma 18. The strictly convex outer polygon from Lemma 14 gives positive signed area to three distinct boundary vertices in that order. Every summand is consequently nonnegative.

Lemma 17 supplies three disjoint paths with distinct roots and a rooted choice extending them. That term has positive weight and positive area. The sum is strictly positive, and $Z > 0$ by Lemma 15. Division by Z proves the claim. □

5. Geometric assembly in the prescribed embedding

Strict support of each facial cycle must imply assertions about the whole drawing: exact incidences, complementary faces and the original cyclic orders. We prove these implications separately. The first lemma is purely geometric and also justifies the outer polygon used in Section 3.

5.1. **A polygon from strict edge supports.** For a cyclic list of distinct points $p_0, \dots, p_{m-1}$, $m \geq 3$, use subscripts modulo m, and define the affine slack functions

$$\ell_i(x) = \det(p_{i+1} - p_i, x - p_i), \qquad K = \bigcap_{i=0}^{m-1} \{x : \ell_i(x) \geq 0\}.$$

The half-planes defining K are closed.

Lemma 20 (Strictly supported polygon)**.** *Assume $\ell_i(p_j) > 0$ whenever $j \notin \{i, i+1\}$. Then K is a bounded convex set with nonempty interior, $\overline{\operatorname{int} K} = K$, and*

$$K \cap \{\ell_i = 0\} = [p_i, p_{i+1}], \qquad \partial K = \bigcup_i [p_i, p_{i+1}].$$

The listed segments, in their cyclic order, form the complete simple counterclockwise boundary of K. Each interior angle is strictly less than π. Moreover, for $x \in (p_i, p_{i+1})$, a neighborhood U of x satisfies

$$U \cap K = U \cap \{\ell_i \geq 0\}, \qquad U \cap \operatorname{int} K = U \cap \{\ell_i > 0\}.$$

Proof. Every listed vertex satisfies every constraint. The average of any three distinct listed vertices has strictly positive slack for every edge: at least one of those three is not an endpoint of that edge. Thus K has a strict feasible point x_*, and hence nonempty interior. It is closed and convex by its definition.

Since the vectors $p_{i+1} - p_i$ sum to zero, the sum $\sum_i \ell_i(x)$ is a constant C, independent of x. It is positive by evaluation at x_*. For $x \in K$, therefore, $0 \leq \ell_i(x) \leq C$ for every i. The edge vectors cannot all be parallel: the hypothesis for p_0, p_1, p_2 already excludes their collinearity. Choose two independent edge vectors. Their slack functions have independent linear parts, so their joint inverse image of $[0, C]^2$ is bounded. It contains K, proving boundedness.

On the line $\ell_i = 0$, write $x = p_i + t(p_{i+1} - p_i)$. The preceding-edge constraint becomes $t\ell_{i-1}(p_{i+1}) \geq 0$, with positive coefficient. The following-edge constraint becomes $(1 - t)\ell_{i+1}(p_i) \geq 0$, again with positive coefficient. Consequently $0 \leq t \leq 1$. Conversely every such t satisfies every constraint, by affine interpolation between the endpoints. This proves the exact-line intersection.

A point of K with all slacks positive is interior, by finiteness and continuity of the constraints. A zero slack places it on a supporting line, so it is a boundary point. Thus the displayed segments exhaust ∂K. A nonconsecutive segment lies strictly on the positive side of an edge's line, because both its endpoints do. Consecutive segments meet only at their common listed endpoint: the three successive vertices have strictly positive turn, so the segments are not collinear. It follows that the prescribed traversal is simple and complete. Its positive-side

interior gives the counterclockwise orientation and its strictly positive turns give strict polygonal convexity.

For any $x \in K$, the point $(1-t)x + tx_*$ has all slacks positive when $0 < t \le 1$. Letting $t \downarrow 0$ proves $\overline{\operatorname{int} K} = K$. Finally, at an open-edge point every constraint other than ℓ_i is strict. This follows by interpolation, since for each other edge at least one endpoint has positive slack. They remain strict in a sufficiently small neighborhood, which proves the asserted local half-plane description. □

Apply this lemma to every bounded facial cycle of the original embedding, using Lemma 19, and to the outer cycle in counterclockwise order, using Lemma 14. Write K_F for the closed body associated with a bounded face F, and K_0 for the outer body. Let

$$\Gamma = \bigcup_{ab \in E(G)} [q(a), q(b)]$$

be the union of all new segments. At this stage, these individual segments have distinct endpoints, but global noncrossing has not yet been established.

5.2. **Tiling and exact incidences.** We use two elementary properties of the original plane graph. Every edge has two distinct incident faces, and each edge and vertex belongs to a bounded facial cycle. The oriented boundaries of all bounded faces, traversed counterclockwise, sum as an edge chain to the counterclockwise outer boundary. These properties hold because G is 2-connected; in particular its facial boundaries are simple cycles and it has no bridges.

Lemma 21 (Closed tiling)**.** *The interiors of the K_F are pairwise disjoint, each K_F is contained in K_0, and*

$$\bigcup_{F \text{ bounded}} K_F = K_0.$$

Proof. For a point $x \notin \Gamma$, the winding number of a simple counterclockwise polygon around x is 1 in its interior and 0 outside its closed body. Winding number is additive under concatenation of directed segment paths, and reversal negates each contribution. These are winding numbers of the new polygonal curves, each already simple by Lemma 20.

In the sum over bounded faces of the original embedding, the two directions of each interior edge cancel. The remaining directed edges are exactly the counterclockwise outer cycle. Hence

$$\sum_{F \text{ bounded}} \mathbf{1}_{\operatorname{int} K_F}(x) = \mathbf{1}_{\operatorname{int} K_0}(x) \qquad (x \notin \Gamma). \tag{12}$$

This uses the original facial edge partition, which is available before the new segments have been shown to form an embedding.

The complement of Γ is dense, since Γ is contained in finitely many lines. An intersection of two distinct polygon interiors would be open and would contain a point outside Γ, contradicting (12). Similarly, an interior point of K_F outside the closed set K_0 would yield an open set of such points and a contradiction. Thus $\operatorname{int} K_F \subseteq K_0$. Taking closures gives $K_F \subseteq K_0$. Conversely (12) puts every point of $\operatorname{int} K_0 \setminus \Gamma$ in some K_F. The finite union of these closed sets is closed; density and $\overline{\operatorname{int} K_0} = K_0$ give the reverse inclusion. □

Lemma 22 (Contact with an open edge)**.** *If $x \in (q(a), q(b))$ for an original edge ab, and $x \in K_F$ for a bounded face F of the original embedding, then ab is a boundary edge of F.*

Proof. Suppose first that ab is not an outer edge. Its two incident bounded faces in the original embedding, say F_1, F_2, traverse it in opposite directions. By the local assertion of Lemma 20, their interiors occupy the two opposite open half-neighborhoods of the edge line near x. More precisely, after intersecting their two neighborhoods, membership in these interiors is characterized by the two strict signs of the same affine slack.

If F were distinct from both F_1, F_2, the relation $K_F = \overline{\operatorname{int} K_F}$ would give interior points of K_F arbitrarily close to x. We can choose such a point off the edge line, because this interior is open. It then belongs to the interior of K_{F_1} or K_{F_2}, contrary to Lemma 21.

If ab is an outer edge, it has one bounded incident face, say F_1. Its interior and the interior of K_0 have the same local open half-plane along this edge. Every K_F is contained in K_0. If $F \neq F_1$ and $x \in K_F$, an interior point of K_F sufficiently close to x, chosen off the line, must therefore lie on the K_0 side. It then lies in $\operatorname{int} K_{F_1}$, again a contradiction. □

Lemma 23 (Exact segment incidences)**.** *No vertex point lies on an edge segment except at its own endpoint, and two distinct original edge segments meet only at images of their common original endpoints.*

Proof. The placement is globally injective, so only open-edge contacts need consideration for the first assertion. Suppose $q(c)$ lies in the open segment of ab, with $c \notin \{a, b\}$. Choose a bounded face F of the original embedding incident to c. Its body contains $q(c)$. Lemma 22 forces ab to be an edge of F. Then a third listed vertex of this polygon lies on that edge, contrary to its strict support.

Now consider a common point x of two distinct edge segments. If x is the image of any original vertex, the first assertion and injectivity identify it as a common original endpoint. Otherwise x lies in the open part of each segment. Choose a bounded face incident to one of the edges. Its body contains x, so Lemma 22 puts the other edge on the same polygon. Lemma 20 excludes an intersection of their open parts, whether the two edges are consecutive or nonconsecutive. This also excludes collinear overlaps. □

5.3. **Complementary faces and the embedding map.**

Lemma 24 (Complementary regions)**.** *The components of* $\mathbb{R}^2 \setminus \Gamma$ *are exactly the sets* $\operatorname{int} K_F$ *and* $\mathbb{R}^2 \setminus K_0$*. The former are the bounded components and the latter is the unbounded component.*

Proof. Every original edge belongs to a bounded facial cycle, and the polygons have precisely their original boundary segments. Therefore

$$\Gamma = \bigcup_{F \text{ bounded}} \partial K_F. \tag{13}$$

For $F \neq H$, an interior point of K_F cannot belong to K_H: since $K_H = \overline{\operatorname{int} K_H}$, its membership would force points of $\operatorname{int} K_H$ inside the open set $\operatorname{int} K_F$. The disjointness in Lemma 21 excludes this. An interior also avoids its own frontier, so (13) shows that every polygon interior avoids all of Γ.

Conversely, if $x \in K_0 \setminus \Gamma$, closed coverage places it in some K_F, and avoidance of its frontier places it in $\operatorname{int} K_F$. All segments lie in K_0. Hence

$$\mathbb{R}^2 \setminus \Gamma = (\mathbb{R}^2 \setminus K_0) \,\dot\cup \coprod_{F \text{ bounded}} \operatorname{int} K_F.$$

Each set in this finite partition is nonempty and open. The polygon interiors are convex and connected. The exterior of the bounded convex body K_0 is path connected: choose an interior point z and a circle centered at z containing K_0 in its interior. An exterior point can move radially outward to this circle without entering K_0; otherwise convexity along its ray from z would place the original point in K_0. Arcs of the circle connect the resulting radial paths. The radius may be chosen large enough for any two specified exterior points.

In a partition into finitely many disjoint open sets, each part is also relatively closed in the union. A connected component can therefore meet only one part. Since each part is connected, it is a full component. Boundedness of K_F and unboundedness of the exterior prove the last assertion. □

Lemma 25 (Prescribed rotation and ambient extension)**.** *The straight drawing has the original cyclic edge order at every vertex and the original outer-face identity. There is an orientation-preserving homeomorphism of* $\mathbb{R}^2$ *carrying the original drawing to this drawing. It can be chosen to carry each parametrized original edge to its straight segment at the same parameter.*

Proof. By Lemma 23, distinct incident edges have distinct initial rays; coincident rays would overlap in an open segment. At a bounded facial corner, the convex sector between its two

boundary rays contains no other ray, because Lemma 24 excludes the graph from that face's interior. The counterclockwise facial traversal therefore gives the same consecutive pair in the cyclic order of the new drawing as in the original embedding. At an outer corner, all segments lie in K_0, so the exterior sector is empty of other rays and gives the corresponding outer-face pair. The facial corners of the original graph exhaust the successive pairs at every vertex. Their orders thus determine exactly the original rotations. Lemma 24 already identifies the selected unbounded face.

It remains to construct the ambient map, rather than infer it from the rotation assertion alone. On the original embedded graph, map each vertex to $q(v)$ and each simple original edge arc, in its prescribed interval parameter, to the affine segment with those endpoints. Exact incidences make this well-defined and injective. It is a homeomorphism of the embedded graphs: on each compact arc it is a homeomorphism, the finitely many maps agree at shared endpoints, and the whole graph is compact.

Every original facial cycle is a Jordan curve. Its graph map is a boundary homeomorphism to the corresponding simple polygon, with matching orientation. The Jordan–Schönflies extension theorem [7, Proposition 1.9] extends each bounded facial boundary homeomorphism to the closed disk it bounds. Apply its planar extension form also to the outer boundary, and retain the resulting map on the closed exterior. This exterior extension maps the unbounded side to the unbounded side. The extended maps agree on all overlaps, since those overlaps are precisely the already matched edge arcs and vertices. Their domains form a finite closed cover of the plane. They therefore paste to a continuous map. The image disks and exterior form the corresponding finite closed cover by Lemma 24; their inverse maps paste in the same way. Thus the map is a homeomorphism. The matching counterclockwise boundary orientations allow orientation-preserving disk extensions and give positive orientation for the pasted planar homeomorphism. The edge parametrizations are preserved because the extensions leave all prescribed boundary maps unchanged. □

Proposition 26 (Facewise assembly)**.** *The placement q is a straight-line drawing with its prescribed embedding and outer face. Its bounded faces are exactly* $\operatorname{int} K_F$*, its outer face is $\mathbb{R}^2 \setminus K_0$, and all facial boundaries are strictly convex polygons.*

Proof. Combine Lemmas 20, 23, 24 and 25. □

6. Euclidean progress and proof of the main theorem

Lemma 27 (metric estimate)**.** *Let h be an injective greedy integer labeling of a finite graph, and let $X : V(G) \to [0, 1/4]$. For $q = (X, h)$ and any distinct s, t, every neighbor a giving strict height progress toward t satisfies*

$$\|q(t) - q(a)\| + \tfrac{3}{4} \le \|q(t) - q(s)\|, \qquad \|q(t) - q(a)\|^2 + 1 \le \|q(t) - q(s)\|^2.$$

Proof. Put $A = |h(t) - h(s)|$ and $B = |h(t) - h(a)|$. These are nonnegative integers with $A \ge B + 1$. The triangle inequality and the strip bound give

$$\|q(t) - q(a)\| \le B + \tfrac{1}{4} \le A - \tfrac{3}{4} \le \|q(t) - q(s)\| - \tfrac{3}{4}.$$

If $B = 0$, injectivity of h gives $a = t$, so the squared-distance decrease is at least $A^2 \ge 1$. If $B \ge 1$, then $A^2 - B^2 \ge 2B + 1 \ge 3$. The difference of the two horizontal squared distances is at least $-1/16$, giving squared-distance decrease at least $3 - 1/16 > 1$. □

Proof of Theorem 1. Choose a clockwise edge uv of the prescribed outer boundary. Corollary 11 supplies a rooted greedy integer labeling with minimum $h(u) = 0$ and maximum $h(v) = T$. Lemma 12 gives the height order on each facial boundary. Choose the positive rows in Section 3 and the boundary data $X(b) = h(b)(T - h(b))/T^2$. Lemma 13 gives a unique rational solution, with $0 \le X \le 1/4$. Both coordinates of $q = (X, h)$ satisfy the interior equations.

Lemma 14 makes the outer polygon strictly convex. The forest identity and the disjoint-path arguments give every bounded facial cycle the strict supports of Lemma 19. Proposition 26 therefore identifies q as the prescribed straight-line plane drawing, with strictly convex facial polygons and an orientation-preserving ambient homeomorphism. Lemma 27, applied to a

height-progress neighbor for each ordered pair, proves both metric inequalities for this same drawing. □

All heights and horizontal coordinates in this construction are rational. The proof is an existence and construction argument; no bound on coordinate bit length or drawing area is asserted here. The constants 3/4 and 1 express the chosen coordinate units, and uniform scaling changes the distance and squared-distance margins accordingly.

7. Formal verification and supporting materials

A formal proof of Theorem 1 is given in Lean 4. Its assumptions are a finite continuous plane embedding and three-connectivity. The formal statement constructs the vertex placement, strictly convex facial polygons, both distance inequalities, and an orientation-preserving homeomorphism carrying the original embedding to the straight-line drawing. It also preserves the parametrization of each original edge.

The formal proof uses Lean 4.32.2, Mathlib, and a formalization of the Jordan–Schönflies theorem. The main theorem depends only on Lean's standard foundational axioms: propositional extensionality, classical choice, and quotient soundness. The exact source and software versions are specified in the linked source snapshot.

The research page collects the paper and supporting materials. The formalization page accompanies an immutable Lean source snapshot, including the module containing the main theorem. The dated PDF of this article and its ProofAtlas works entry provide permanent references to this version and to the result.

Acknowledgments and AI assistance

The author thanks the developers of Lean and Mathlib and the authors of the structural and topological results used in the proof.

The ProofAtlas.ai harness was used for the AI-assisted research and verification workflow. OpenAI GPT-6 Pro and Codex contributed substantially to mathematical exploration, proof development, computational testing, Lean formalization and exposition. Lech Mazur directed the research and is responsible for the manuscript and its claims. AI output is not itself proof evidence: the mathematical claims are supported by the arguments and the accompanying Lean formalization.

References

[1] S. Chaiken, *A combinatorial proof of the all minors matrix tree theorem*, SIAM Journal on Algebraic and Discrete Methods 3 (1982), no. 3, 319–329. https://doi.org/10.1137/0603033.

[2] G. Da Lozzo, A. D'Angelo and F. Frati, *On planar greedy drawings of 3-connected planar graphs*, 33rd International Symposium on Computational Geometry, LIPIcs 77 (2017), 33:1–33:16. https://doi.org/10.4230/LIPIcs.SoCG.2017.33. We use Definition 4 and Lemmas 5–6 of the full version, arXiv:1612.09277v2 (2 January 2017), https://arxiv.org/abs/1612.09277v2.

[3] R. Diestel, *Graph Theory*, fifth edition, Graduate Texts in Mathematics 173, Springer, 2017. https://doi.org/10.1007/978-3-662-53622-3.

[4] J. Erickson and P. Lin, *Planar and toroidal morphs made easier*, arXiv:2106.14086v2 (26 August 2021). https://arxiv.org/abs/2106.14086v2.

[5] M. S. Floater, *Parametric tilings and scattered data approximation*, International Journal of Shape Modeling 4 (1998), nos. 3–4, 165–182. https://doi.org/10.1142/S021865439800012X.

[6] T. Leighton and A. Moitra, *Some results on greedy embeddings in metric spaces*, 49th Annual IEEE Symposium on Foundations of Computer Science, 2008, 337–346. Author manuscript: https://people.csail.mit.edu/moitra/docs/greedy-routing.pdf.

[7] C. Ó Dúnlaing, *Nodally 3-connected planar graphs and convex combination mappings*, arXiv:0708.0964v1 (7 August 2007). https://arxiv.org/abs/0708.0964v1.

[8] C. H. Papadimitriou and D. Ratajczak, *On a conjecture related to geometric routing*, ALGOSENSORS 2004, Lecture Notes in Computer Science 3121, 9–17. https://doi.org/10.1007/978-3-540-27820-7_3.

[9] W. T. Tutte, *How to draw a graph*, Proceedings of the London Mathematical Society, Series 3, 13 (1963), 743–767. https://doi.org/10.1112/plms/s3-13.1.743.

Email address: 2022melodies@gmail.com